2016 IEEE Radar Conference (RadarConf)

Enhancing Spectrum Coexistence using Radar Waveform Diversity

Mark A. Govoni, *Senior Member, IEEE*
Aberdeen Proving Ground, MD, USA

***Abstract*— In an effort to meet the growing demands of the mobile communications industry, the recent Federal Communications Commission (FCC) auction of the 1695-1710 & 1755-1780 MHz bands marked the continued commitment by regulators to make available frequencies previously reserved for the military to the general public. While good for the economy, the Advanced Wireless Services (AWS-3) auction presents unprecedented challenges for incumbent military systems. In particular, the manner in which military radar systems are required to share spectrum represents a sharp contrast to how spectrum was previously accessed. Military radar systems, whether directly affected by the auction or yet to be designed, are expected to utilize innovative spectrum sharing technologies to meet the demand of this new paradigm. In this paper, the research is motivated by the aforementioned challenges and focuses on how the benefits of waveform diversity could serve as a potential solution to enhancing spectrum coexistence for military radar systems.**

***Index Terms*— spectrum coexistence, radar waveform diversity, interference protection criteria (IPC), frequency dependent rejection (FDR)**

I. Introduction

The ability for military radar and commercial broadband devices to operate on a coordinated basis is becoming more of a necessity as the commercial demand for spectrum grows and consequently, as military exclusivity diminishes. Previous research has grown our understanding of the benefits of radar waveform diversity and how it minimizes the effects of interference on narrowband communications receivers [1], [2]. Independent research on cognitive radar technology has agreed that a spectrum resource manager providing a priori knowledge to in-band users is necessary for enhancing coexistence [3], [4]. Also showing promise is multi-objective optimization, a technique that attempts to limit radar interference by restricting emissions in specific bands [5], [6].

In order to further assess the value-added of waveform diversity, the interference protection criteria (IPC) is established and evaluated under the assumption of a non-fading (no multipath or obfuscation) RF channel for the case of an interference-limited system consisting of a radar and a "victim" communications system. Interference is determined by numerically evaluating the international definition for frequency dependent rejection (FDR) [7]. In the analysis, the author considers the inclusion of waveform diversity as an added degree of freedom available to the radar system. In doing so, insight into how radar interference can be dynamically managed without causing *a)* the communications system to exceed allowable performance degradation limits, *b)* frequency discontinuities in the radar transmit spectrum, and *c)* significant degradation to radar performance.

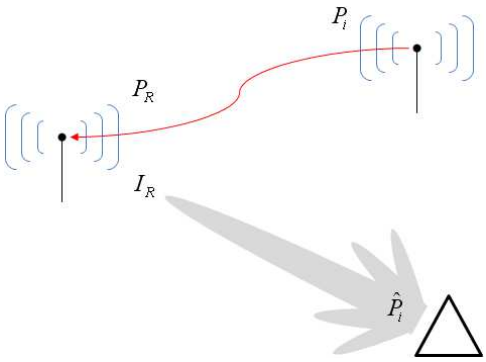

Fig. 1. Spectrum coexistence scenario for radar and communications network.

II. System Model

A. Radar-to-Communications Interference

The scenario under consideration consists of a ground surveillance radar that is periodically scanning over a predetermined search volume. At some point within the radar search interval, the spatial extent of the radar power aperture coincides with a communications network consisting of multiple nodes, each of which are communicating with other nodes within the radar search volume. Figure 1 depicts the instance when the radar and communications node are spatially aligned and represents the greatest likelihood for interference.

The physical model for determining interference for this situation is described by first defining the incident power density radiated by the communications node as

$$P_i = \frac{P_T G_{tx}}{4\pi R^2}, \tag{1}$$

where P_T is the omni-directional transmit power from the communications node, G_{tx} is the node transmit gain, and R is the distance between communications nodes. It follows that the desired receive power is defined as

$$\begin{aligned} P_R &= P_i A, \\ &= \frac{P_T G_{tx} G_{rx}}{\left(\frac{4\pi f R}{c}\right)^2}, \end{aligned} \tag{2}$$

where A is the node antenna area, G_{rx} is the node receive gain, c is the speed of light, and f is the communications system center frequency. By inspection of (2), the signal-to-noise ratio (SNR) is simply $P_R/\mathcal{N}$, where $\mathcal{N}$ is the communications receiver sensitivity comprised of the noise figure and the band-limited, thermal noise. Next, the author defines the incident power density radiated by the radar towards the communications node as

$$\hat{P}_i = \frac{\hat{P}_T \hat{G}_{tx}}{4\pi \hat{R}^2}, \tag{3}$$

where $\hat{P}_T$ is the directional transmit power from the radar, $\hat{G}_{tx}$ is the radar transmit gain, and $\hat{R}$ is the distance between the radar and the communications node. The interference experienced by the communications node from the radar is then defined as

$$\begin{aligned} I_R &= \hat{P}_i A, \\ &= \frac{\hat{P}_T \hat{G}_{tx} G_{rx}}{\left(\frac{4\pi \hat{f} \hat{R}}{c}\right)^2}, \end{aligned} \tag{4}$$

where $\hat{f}$ is the radar center frequency. By inspection of (4), the interference-to-noise ratio (INR) is simply $I_R/\mathcal{N}$, where again, $\mathcal{N}$ is the communications receiver sensitivity.

B. Interference Protection Criteria

Because our communications receiver is functioning as an interference-limited system, the conventional IPC is best defined by the signal-to-interference ratio (SIR). The SIR is simply the ratio between the desired receive power and the undesired radar interference, represented by (2) and (4), respectively. After removing like-terms, the SIR in decibels is defined as

$$\text{SIR} = P_T + G_{tx} - L_p - \hat{P}_T - \hat{G}_{tx} + \hat{L}_p, \tag{5}$$

where L_p is the path loss between communications nodes and $\hat{L}_p$ is the path loss for the radar-to-communications node. Intuitively, interference is deemed unacceptable when the communications receiver experiences interference in excess of the desired receive power. Therefore, the recommended distance in which a radar can safely operate without causing interference to the communications receiver must satisfy the IPC such that the SIR $\geq$ IPC.

Figure 2 is a plot of the SIR described in (5) and is evaluated with varying communications node-to-node distances. The author assumes the communications system is always operating below the radar height $\hat{h}$. Therefore, the radar horizon, $R_z = \sqrt{2\hat{h}\frac{4}{3}r_e}$, represents the maximum achievable line-of-sight distance in the analysis. From the figure, it is observed that when the node-to-node distance is less, the SIR is higher since the receive power is greater. Similarly, the SIR will improve when higher radar frequencies are used since the radar path loss will be greater. It's worth mentioning that when the communications receiver functions as a noise-limited system, the International Telecommunication Union - Radiocommunication Sector (ITU-R) recommends an INR of -6 dB or less to ensure minimal impact to the communications receiver [8]–[11].

C. Waveforms

The author next discusses the conventional and non-conventional pulse compressed radar waveforms used in the research. It is assumed that the primary objective of the radar system facilitating these waveforms is to maximize detection performance and maintain resolution while minimizing interference for other in-band systems. Since the author considers peak interference in the analysis, it's assumed that the radar system operates in a pulsed manner.

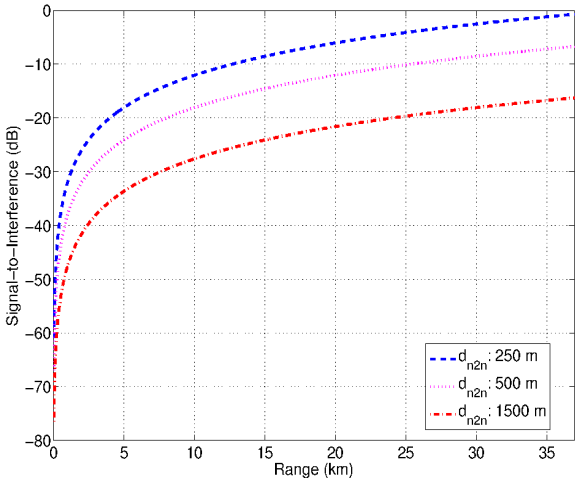

Fig. 2. SIR as a function of the distance from radar to communications node for varying node-to-node distances. P_T = 37 dBm, $\hat{P}_T$ = 65 dBm, G_{tx} = 2 dBi, $\hat{G}_{tx}$ = 19 dBi, $f = \hat{f}$ = 1300 MHz, $\hat{h}$ = 80 m AGL, and R_z = 37 km.

The linear frequency modulation (LFM) chirp waveform has a time-bandwidth product that is much larger than unity. This characteristic can be quantified, and is typically referred to as the pulse compression gain. With digital signal processing, the benefits of large bandwidths are realized without having to transmit extremely narrow pulses. The baseband, discrete-time equivalent of a complex LFM chirp signal is defined as

$$\begin{aligned} s[n] &= \cos \pi \mu n^2 + j \ \sin \pi \mu n^2 \\ &= e^{j\pi\mu n^2}, \ k = 1 \ldots N \end{aligned} \tag{6}$$

where μ is the chirp rate, $n = \frac{t}{T_s}$ is the discrete-time index, $T_s = \frac{\tau}{N}$ is the sampling period with pulse duration τ, and $s[n]$ is one of $N = 2^{\lceil \log_2(\tau\beta) \rceil}$ time samples. The unweighted, matched filter (MF) output for the chirp LFM waveform is a sinc-function having an approximate peak-to-sidelobe ratio (PSLR) of -13 dB. In the analysis, a 4^{th}-order Taylor window provides the necessary weighting to meet a sidelobe specification of -18 dB PSLR and -30 dB integrated sidelobe ratio (ISLR).

In addition to the LFM waveform, a PM waveform in the form of a biphase code is also considered. A Barker code having comparable resolution to the chirp LFM is chosen. To achieve this, a nested Barker code $\{b_7 \otimes b_{11}\}$ is formed, zero-padded, and replicated over a sequence of 1024-pts. The weighted, MF output for the nested Barker code is shown in Figure 3 and includes the output of the LFM for reference. From the figure, the nested Barker code exhibits peak sidelobes that are $1/7^{th}$ of the $-20\log_{10} 77$ theoretical value.

For the cases of non-conventional waveforms, the author's definition of non-conventional refers to waveforms whose characteristics, through direct digital synthesis, are re-programmable as a means of compensating for diminishing channel conditions e.g. interference. Specifically, the non-conventional waveforms used in this research employ interference mitigation techniques that either impose constraints on radar transmit power through amplitude modulation (AM) or they spread the radar spectrum over a very wideband through phase modulation (PM). Both waveforms

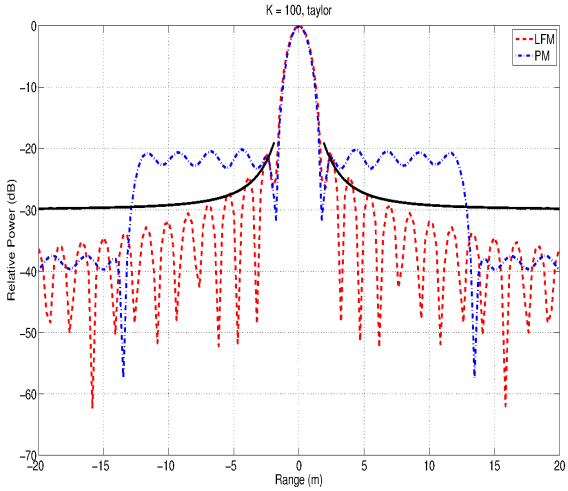

Fig. 3. MF ouput for nested Barker sequence ($b_7 \otimes b_{11}$). 100 pulses, Taylor weighting. *Note:* Solid line represents sidelobe specification

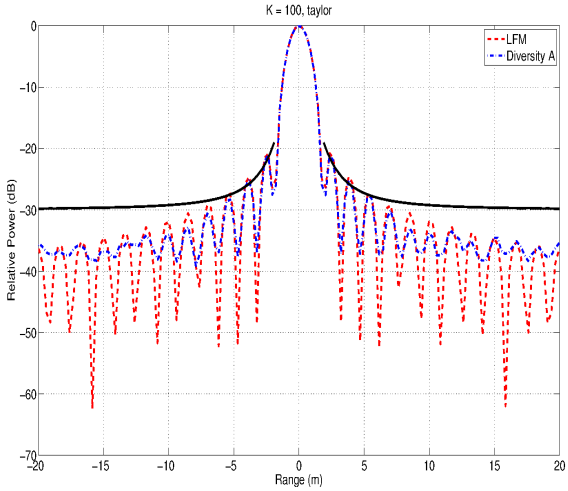

Fig. 4. MF ouput for APCNa10k00 (α = 1, κ = 0). 100 pulses, Taylor weighting. *Note:* Solid line represents sidelobe specification

are designed in a manner that allow them to achieve similar performance to the two previously-discussed radar waveforms.

As such, the radar waveform of choice is advanced pulse compression noise (APCN) [12], [13]. To help in understanding APCN, the baseband, discrete-time equivalent of a complex, stochastic signal is defined as

$$\begin{aligned} g[n] &= A_n \cos\vartheta_n + j\ A_n \sin\vartheta_n \\ &= A_n e^{j\vartheta_n},\ n = 1 \ldots N \end{aligned} \tag{7}$$

where $A_n \sim |\mathcal{R}(1)| \in [1-\alpha, 1]$ is a Rayleigh-distributed random variable whose range is controlled by α, and $\vartheta_n \sim \mathcal{U}(0, 2\pi) \in [0, 2\pi\kappa]$ is a uniformly-distributed random variable whose range is controlled by κ. By taking the Hadamard (element-wise) product of (6) and (7), the APCN waveform is defined as

$$\begin{aligned} v[n] &= s[n] \circ g[n] \\ &= A_n e^{j\{\pi\mu n^2 + \vartheta_n\}},\ n = 1 \ldots N \end{aligned} \tag{8}$$

where (8) also serves as the impulse response $h[n]$ to the LTI system. Two APCN radar waveforms are considered. The first is the AM case, referred to as "Diversity A", where α is set to 1 giving the waveform synthesizer the freedom to choose from the full-range of internally-generated, Rayleigh-distributed random variables. The second is the PM case, referred to as "Diversity B", where κ is set to 0.7 giving the waveform synthesizer the freedom to choose from 70% of the full-range of internally-generated, uniformly-distributed random variables. It should be noted that even though the author is defining two specific APCN waveforms, hundreds of combinations exist for $0 \leq \{\alpha, \kappa\} \leq 1$. The behavior of the many different APCN waveforms is distinguishable, and therefore, will have different radar ambiguity functions as well.

Signal processing of the APCN waveform begins with the input signal $x[n] = v^*[n-\eta]$. The transform of the impulse response $h[n] = v[n] \Leftrightarrow V(e^{j\omega})$ serves as the matched filter to the system. The transform of the input signal $v^*[n-\eta] \Leftrightarrow V^*(e^{-j\omega})e^{-j\omega\eta} \equiv V^*(e^{j\omega})e^{j\omega\eta}$ because of Fourier symmetry. By combining the two transforms, $Y(e^{j\omega}) = V(e^{j\omega})V^*(e^{j\omega})e^{j\omega\eta}$, the product results

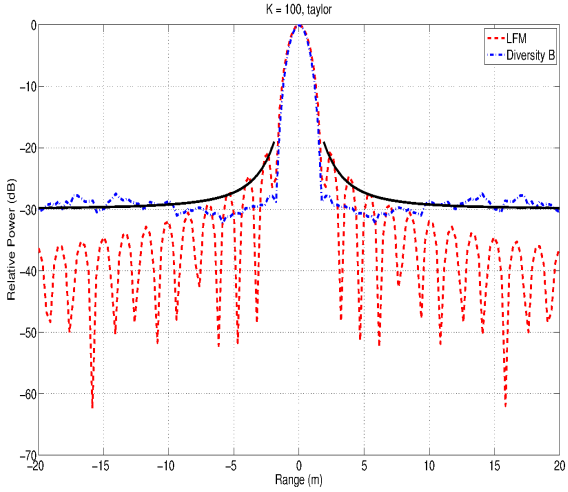

Fig. 5. MF ouput for APCNa00k07 (α = 0, κ = 0.7). 100 pulses, Taylor weighting. *Note:* Solid line represents sidelobe specification

in the matched filter output by way of the Wiener-Khintchine theorem

$$y[n] = \frac{1}{2\pi} \sum_{n=0}^{N-1} |S_{VV}(e^{j\omega})|^2\ e^{j\omega n}, \tag{9}$$

where $|S_{VV}(e^{j\omega})|^2 \equiv V(e^{j\omega})V^*(e^{j\omega})$ is the power spectral density (PSD). The weighted, MF output for the two APCN waveforms are shown in Figures 4 and 5, respectively. It is apparent that the APCN waveforms, even though statistically-random by design, exhibit well-behaved sidelobes relative to the predetermined specification.

The author briefly mentions the communications signal next. Quadrature AM (QAM) is very popular in the commercial communications industry because of its simplicity and reliability. In general, higher-order QAM schemes can deliver more data less reliably than lower-order QAM scheme, and to keep the bit error rate at a minimum, requires more SNR.

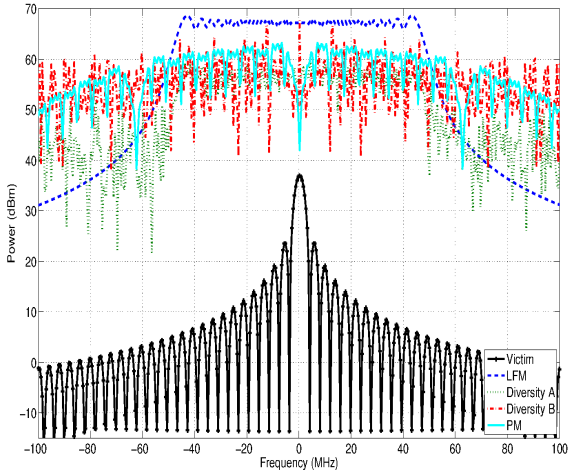

Fig. 6. PSD for radar waveforms and communications signal. B = 5 MHz and $\hat{B}$ = 100 MHz

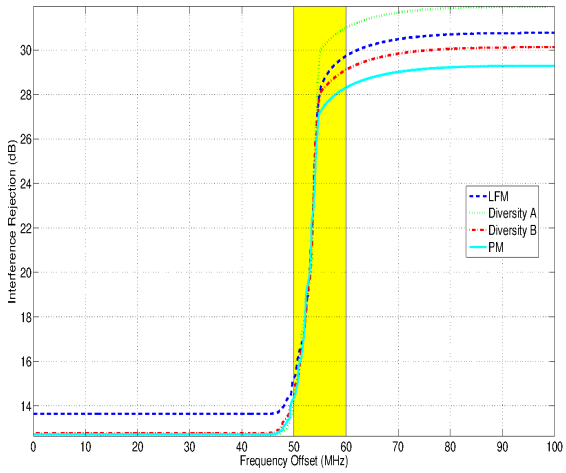

Fig. 7. Interference rejection for communications receiver. B = 5 MHz, and $\hat{B}$ = 100 MHz. *Note:* Shaded area indicates transition region between OTR and OFR(Δf)

In the analysis, the author considers an 4-QAM scheme that conveys binary data in the form of $\lceil \log_2(4) \rceil$ bits per symbol by modulating the amplitudes of two carrier waves using amplitude-shift keying. 4-QAM is less susceptible to interference relative to higher-order QAM schemes, and therefore makes for an interesting test case. The transmitted signal for QAM is

$$z[n] = I[n] \cos 2\pi f_0 n - Q[n] \sin 2\pi f_0 n, \quad n = 1 \dots N \tag{10}$$

where $I[n]$ and $Q[n]$ are the in-phase and quadrature components of the signal, $n = \frac{t}{T_s}$ is the discrete-time index, and $T_s = \frac{\tau}{N}$ is the sampling period with pulse duration τ. A raised-cosine filter (β = 0.75) is used for pulse-shaping. The power spectrum for the communications signal having bandwidth B and radar waveforms having bandwidth $\hat{B}$ is shown in Figure 6. The reader should note that the values plotted represent peak power and not the power described in (2) and (4).

III. Interference Analysis

A. Frequency Dependent Rejection

In general, the effects of interference are determined by measuring the total power through the communications receiver and *not* just measuring the power at the receiver. In doing so, one is able to estimate the communications receiver's ability to reject interference as a function of filter mismatch and frequency offset. These two metrics, referred to as the on-tune rejection (OTR) and off-frequency rejection (OFR), are useful for evaluating interference rejection by the communications receiver [9]–[11].

In this respect, the FDR can be viewed as a system gain for the communications receiver. Furthermore, if the interference experienced by the communications receiver is a quantity available to the radar system, it's conceivable that waveform diversity could be used to expedite compliance with the established IPC. Considering the desired receive power and the undesired radar interference, the expression for FDR is

$$\text{FDR}(\Delta f) = 10 \log_{10} \left[\frac{\int_{-\infty}^{\infty} V(f) df}{\int_{-\infty}^{\infty} V(f) \cdot Z(f + \Delta f) df} \right], \tag{11}$$

where $V(f)$ is the PSD of the radar interference, $Z(f)$ is the frequency response of the communications receiver, $\Delta f = \hat{f}_c - f_c$ is the frequency offset. For positive frequencies, the two systems are considered out-of-band when the offset equals the larger of the two system bandwidths, in this case, the radar bandwidth. The boundaries for FDR are defined as

$$\text{FDR}(\Delta f) = \begin{cases} \text{OTR}, & \Delta f \leq B + \hat{B}/2 \\ \text{OFR}(\Delta f), & \text{else.} \end{cases} \tag{12}$$

Interference rejection for the four radar waveforms introduced in the previous section are evaluated and plotted in Figure 7 as a function of frequency offset. From the figure, the LFM waveform has an advantage over the other waveforms in the OTR region of the plot where the communications receiver achieves an OTR of 13.6 dB. This is likely due to a flat spectrum vice what is observed in the remaining waveforms where the mean OTR is 12.7 dB. In the transition region (shaded area), the performance between all waveforms tends to converge. And finally, the effects of radar waveform sidelobes on communications receiver rejection can be seen in the OFR region of the plot. In this region, Diversity A separates itself from the remaining waveforms and offers the greatest reciprocation to communications receiver rejection. At the maximum, the communications receiver OFR for the case of Diversity A is 31.9 dB. For LFM, Diversity B, and PM, the calculated OFR is 30.8 dB, 30.1 dB, and 29.3 dB, respectively. As a reminder, the APCN waveform is easily optimized to behave identically to the LFM waveform. In the event that radar interference is either within the OTR region or out-of-band entirely, the author does not advocate the use of radar waveform diversity as it has the potential to incur unnecessary trade-offs in radar performance [14].

B. Compliance

Three node-to-node distances were considered when evaluating the SIR shown in Figure 2. In this section, we focus on the case when the distance is 1500 meters. This represents the most

difficult of the three cases since the path loss experienced by the communications nodes is the greatest. From the same plot, we can see that greater node-to-node separations translate to lower SIR. Consequently, for tolerable radar interference, the power described in (4) must be reduced by an amount that is compliant with the IPC such that $I'_R = I_R - \text{IPC} + \text{SIR}$, where I'_R is the required interference power for some radar "safe" distance.

In the previous section, the author established FDR as a system gain. In continuing with this assumption, the burden to reduce radar interference power can be relaxed as a function of the communications receiver's ability to reject interference. In this respect, the required interference power becomes $I'_R = I_R - \text{FDR}'(\Delta f)$, where $\text{FDR}'(\Delta f)$ is the required interference rejection necessary for ensuring tolerable radar interference. Presumably, if this modified power requirement were made available to in-band users, the likelihood for interference would be lower thereby enhancing spectrum co-existence.

The required rejection for the case of the four radar waveforms is shown in Figure 8 and plotted against radar safe distances. Intuitively, as the radar moves further away, the interference power lessens, which in turn, lowers the required rejection for the communications receiver. The safe distances corresponding to the four radar waveforms are easily extrapolated from the required rejection curve and are annotated for convenience. It was determined earlier that Diversity A offers the greatest reciprocation to the communications receiver rejection in the OFR region. This is confirmed by Figure 8 where it can be seen that interference corresponding to Diversity A is tolerated at closer distances to the communications system. From Figure 8, Diversity A affords a safe distance of 19.3 km. For LFM, Diversity B, and PM, the extrapolated safe distances are 22.1 km, 23.8 km, and 26.2 km, respectively.

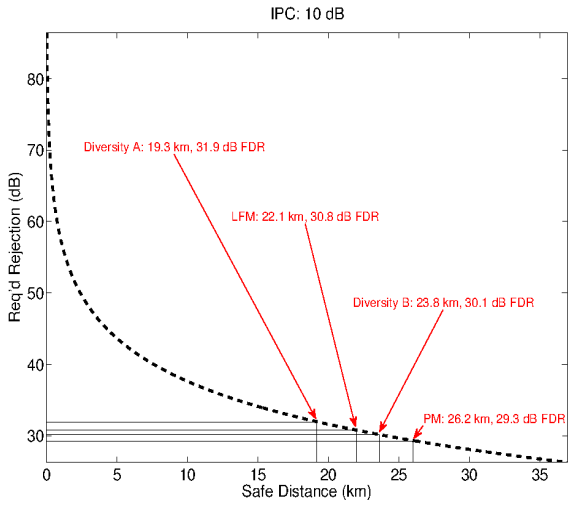

Fig. 8. Required interference rejection and corresponding radar safe distances. 10 dB IPC, 1500 m node-to-node distance, and R_z = 37 km

IV. Conclusions

In this paper, the radar-to-interference model is established for the situation describing interference between a narrowband communications network and a ground surveillance radar. The IPC is established under the assumptions of an interference-limited condition, and in doing so, the SIR relating to the radar-to-interference model is provided. Four different radar waveforms have been evaluated with consideration for how radar interference can be dynamically managed without causing *a)* the communications system to exceed allowable performance degradation limits, *b)* frequency discontinuities in the radar transmit spectrum, and *c)* significant degradation to radar performance. Interference rejection revealed that radar waveform diversity offers the greatest reciprocation to communications receiver rejection.

Acknowledgements

This research was funded by the DARPA Strategic Technology Office (STO) under the Shared Spectrum Access for Radar and Communications (SSPARC) program. The author would like to thank Dr. Jeffrey Boksiner, Dr. Anthony Martone, Joseph Deroba, and Stevan Jovancevic for their insightful comments.

References

[1] H. He, P. Stoica, and J. Li, "Waveform Design with Stopband and Correlation Constraints for Cognitive Radar", 2^{nd} *International Workshop on Cognitive Information Processing*, pp. 344-349, Italy, June 2010.

[2] M. A. Govoni and R. A. Elwell, "Qualitative analysis of interference on receiver performance using advanced pulse compression noise (APCN)", SPIE Defense, Security, and Sensing Conference, vol. 9461, no. 34, May 2015.

[3] A. Aubry, et al., "Cognitive Radar Waveform Design for Spectral Coexistence in Signal-Dependent Interference", *IEEE International Radar Conference*, pp. 474-478, May 2014.

[4] Y. Zhao, J. Gaeddert, K. Bae, and J. Reed, "Radar Environment Map-enabled Situation-aware Cognitive Radio Learning Algorithms", *Proceedings of Software Defined Radio Technical Conference*, Orlando, FL, November 2006.

[5] D. Ciuonzo, A. De Maio, G. Foglia, and M. Piezzo, "Intrapulse Radar-Embedded Communications via Multiobjective Optimization", *IEEE Trans. on Aerospace & Electronic Systems*, vol. 51, no. 4, pp. 2960-2974, October 2015.

[6] A. Martone, M. Govoni, C. Dietlein, K. Sherbondy, and R. Pulskamp, "Tuning Technology for Adaptable Radar Bandwidth", *IEEE International Microwave Symposium*, May 2016.

[7] http://ntiacsd.ntia.doc.gov/msam/FDR/FDR_PROGRAM.doc

[8] ITU-R M.1460, "Technical and operational characteristics and protection criteria of radio determination radars", R00-SG05, March 2006, http://www.itu.int

[9] *Frequency and Distance Separations*, ITU-R Std. SM.337

[10] ITU-R M.1461-1, "Procedures for determining the potential for interference between radars operation in the radio determination service and system in other service", R00-SG08, June 2003, http://www.itu.int

[11] ITU-R M.1464-1, "Characteristics of and protection criteria for radionavigation and meteorological radars operating in the frequency band 2700-2900 MHz", R00-SG08, June 2006, http://www.itu.int

[12] M. A. Govoni, "Linear Frequency Modulation of Stochastic Radar Waveform", Ph.D. dissertation, Stevens Institute of Technology, Hoboken, NJ, April 2011.

[13] M. A. Govoni and R. A. Elwell, "Radar Spectrum Spreading using Advanced Pulse Compression Noise (APCN)," *IEEE Radar Conference*, no 9423, May 2014.

[14] M. A. Govoni and L. R. Moyer, "Preliminary Performance Analysis of the Advanced Pulse Compression Noise Radar Waveform", SPIE Defense, Security, and Sensing Conference, vol. 8361, no. 41, May 2012.